Adaptive-Robust Control of Hybrid Robot Manipulator

Omur Can Ozguney*, Recep Burkan*

**Department of Mechanical Engineering, Faculty of Engineering, Istanbul University-Cerrahpasa, 34320 Istanbul, Turkey (omur.ozguney@iuc.edu.tr, burkanr@iuc.edu.tr)*
**omur.ozguney@iuc.edu.tr (Corresponding Author)*

Abstract: The mobility of robots with rigid links is more limited than that of robots with flexible links. High-mobility manipulators are particularly required in industrial applications. However, mathematical modeling and control of flexible-link robots are challenging. To overcome these difficulties, a hybrid model was considered. The proposed hybrid model consists of a robot with one flexible link and one rigid link. In this study, an adaptive control approach was applied to the hybrid manipulator. The stability of the adaptive controller is ensured by Lyapunov theory. The mathematical structure of the developed controller was designed to be compatible with robotic systems. The applied controller exhibits robustness against external disturbances and system uncertainties. Simulation results demonstrate that the performance of the developed controller is satisfactory

Keywords: Hybrid manipulator, Adaptive control, Lyapunov theory, Robust control, Flexible link

1. INTRODUCTION

1.1 Background

Nowadays, most robots are required to operate with high accuracy in end-point positioning and trajectory tracking. In rigid-link robots, the joints connecting the links are typically heavy, and as a result, a significant portion of the motor torque is consumed to move these joints. Due to these drawbacks, the application areas of rigid robots are gradually decreasing, and they are increasingly being replaced by robots with flexible links. Flexible-link robots, owing to their structural characteristics, require less material, are lighter in weight, consume less power, require smaller actuators, and exhibit higher maneuverability. However, due to the challenges associated with link flexibility and accurate end-point positioning, the industrial adoption of manipulators with fully flexible links has remained limited. Therefore, there is a need for robotic systems that combine both rigidity and flexibility. In this context, the present study investigates a manipulator consisting of one flexible link and one rigid link.

1.2 Literature review

In this study, a hybrid robot manipulator with flexible links is investigated to address control challenges arising from structural flexibility and dynamic uncertainties. The system is modeled using the Euler-Bernoulli beam theory to account for link deflection and angular deformation, and an adaptive-robust control strategy is developed accordingly. Although the proposed structure does not directly correspond to conventional industrial robots such as SCARA, it provides a simplified yet representative platform for validating advanced control algorithms applicable to lightweight, flexible, and human-interactive robotic systems, such as those found in biomedical, wearable, and space applications. The simulation environment is based on MATLAB/Simulink and simulation scenarios are designed to verify the performance and robustness of the control approach. This work aims to contribute to the ongoing research on flexible-link robotic systems by providing a validated control framework that can be extended to more complex real-world applications.

(Book, 1990) determined the mathematical parameters used in modeling flexible links and then examined the systems formed by combining flexible links. (Dwivedy et al., 2006) published a comprehensive literature review examining the methods used in modeling elastic robot manipulators, together with their advantages and disadvantages. (Khairudin et al., 2010) obtained the dynamic model of a two-linked elastic robot arm using the Euler-Lagrange method and examined the behavior of the model under the influence of load. (Chen, 2001) obtained the dynamic behavior of an elastic two-linked planar robot arm by applying the Euler-Bernoulli beam method. (Hayta et al., 2013) examined the closed-loop position control of flexible limb manipulators using PI type fuzzy logic in their study. They compared their results with the results obtained from the LQR control. (Choi et al., 1995) applied the sliding mode control rule to a single-link flexible manipulator. They examined the displacement and torque results obtained from the computer simulation. (Mallikarjunaiah et al., 2013) tried to change the end point of a single-linked elastic robot model with a PID controller. They modeled the dynamic model in accordance with Euler-Bernoulli beam theory. They observed that the results were partially satisfactory. (Akyüz et al., 2010) designed, produced and controlled a single, flexible connected robot arm with a fuzzy controller in their study. There are three different controllers in the fuzzy controller scheme of the flexible connected robot arm. The first controller controls the motor rotation angle; the second controller controls the vibration amount of the end function. The third controller combines the outputs of these two controllers and produces the control signal to be applied to the motor. (Yağız et al., 2001) applied a sliding mode controller to a planar flexible robot arm in their study. In the first part of the study, the mathematical model of the system was created. In the second part, a chattering-free sliding mode control element was applied to the system and the results were examined. (Gee et al., 1997) modeled a single-link elastic manipulator using the finite element method and Lagrange's principle in their article. The manipulator is modeled in accordance with the Euler-Bernoulli beam model and considering that there is a mass at its end point. Then, they developed a nonlinear feedback controller and examined the displacement of the tip point. Recent studies have introduced advanced control strategies for flexible or soft robotic manipulators under various uncertainties and operational constraints. (Chen et al., 2025) proposed an adaptive controller for flexible manipulators with unknown hysteresis and intermittent actuator faults, ensuring stability despite significant nonlinearities. Similarly, (Ma and Liu, 2024) developed an adaptive force control approach with vibration suppression for constrained flexible manipulators facing unknown control directions and time-varying actuator faults. (Li and Liu, 2023) further explored boundary control methods using Nussbaum-type functions to manage similar challenges in distributed-parameter flexible systems.

While these approaches make significant contributions, most are designed either for fully flexible or soft robotic structures or focus on specific issues such as actuator faults or unknown input directions. In contrast, the present study targets hybrid manipulator systems with both flexible and rigid links, and proposes a unified adaptive-robust control scheme that ensures tracking performance and robustness under model uncertainties and external disturbances—an area less explored in recent literature.

Although Lyapunov-based adaptive-robust control methods are well established in the literature, the novelty of this work lies in developing a control strategy specifically tailored for a hybrid manipulator system consisting of both flexible and rigid links. Such hybrid structures present unique challenges in dynamic modeling and control, which are not sufficiently addressed in studies focusing solely on either fully rigid or fully flexible systems. Our approach unifies these two link types under a single control framework, effectively managing their coupled dynamics while ensuring robustness against parametric uncertainties and external disturbances.

In next sections, we provide a systematic derivation of the dynamic model and the proposed control strategy for the hybrid manipulator. Each modeling step and design choice is explained in detail to ensure clarity and reproducibility. Key variables are defined, and the mathematical formulation is structured in a way that allows for straightforward extension to more complex systems.

2. MODELLING

2.1 Dynamics model of a hybrid manipulator

The model shown in Figure 1 was taken as basis and the control system was designed taking this model into consideration. A number of assumptions were accepted when creating the model (Wit, 2014). These are;

1. The model moves only in the horizontal plane.

2. Links are considered as uniform flexible beam.

3. Euler-Bernoulli approach was adopted, and shear stresses and rotational moments of inertia were neglected.

4. It is accepted that there are minor changes in the links.

5. Atmospheric drift effects are ignored.

6. Coulomb friction effect is neglected.

7. The x-direction components of the flexible link are neglected.

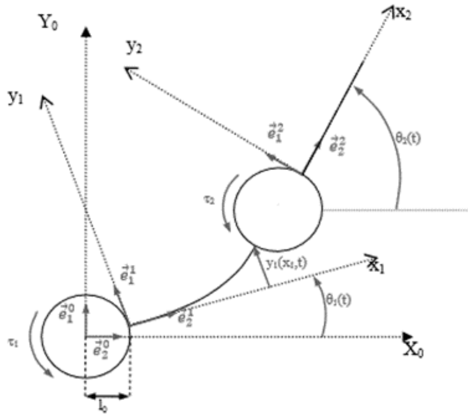

Fig. 1. One link flexible one link rigid robot arm (Wit, 2014).

The manipulator consists of a flexible link modeled using the Euler-Bernoulli beam theory and a rigid link governed by standard rigid-body dynamics. Lagrange formulation was used to obtain the equations of motion of the model. In order to apply the Lagrange method, both the kinetic and potential energy of the system must be determined. For a two-link system, potential energy consists only of the elastic energy of the first link. Potential energy is given in Equation 1 (Wit, 2014). In this step, the kinetic and potential energy of each link is derived separately. The flexible link is treated as a distributed parameter system, and its deflection is expressed using modal coordinates.

$$U_1 = \frac{1}{2}\int_0^{l_1} EI_1 \left(y_1''(x_1,t)\right)^2 dx_1 \tag{1}$$

Kinetic energy consists of the translational and rotational movements of the first and second links.

$$T = T_{t_1} + T_{t_2} + T_{r_1} + T_{r_2} \tag{2}$$

$$T_{t_1} = \frac{1}{2}\int_0^{l_1} \rho_1 \dot{\vec{r}}_1^2 d\,x_1 \tag{3}$$

$$T_{t_2} = \frac{1}{2} m_{H_2} \dot{\vec{r}}_{H_2}^2 + \frac{1}{2} m_2 \dot{\vec{r}}_2^2 \tag{4}$$

$$T_{r_1} = \frac{1}{2} I_{z_1} \dot{\theta}_1^2 \tag{5}$$

$$T_{r_2} = \frac{1}{2} I_{z_2} \dot{\theta}_2^2 \tag{6}$$

$\dot{\vec{r}}_1^2$, $\dot{\vec{r}}_2^2$, refers to the squares of the velocities of the first and second links. (Wit, 2014)

The Lagrange function is as in Equation 7.

$$L=\frac{1}{2}m_{s_1}s_1^2\dot{\theta}_1^2+\frac{1}{2}m_{s_1}\dot{s}_1^2+\frac{1}{2}I_{t_1}\dot{\theta}_1^2+\frac{1}{2}I_{t_2}\dot{\theta}_2^2+m_{\dot{s}_1\dot{\theta}_1}\dot{s}_1\dot{\theta}_1$$
$$+m_{\dot{s}_1\dot{\theta}_2}(\theta_1,\theta_2)\dot{s}_1\dot{\theta}_2+m_{\dot{\theta}_1\dot{\theta}_2}(\theta_1,\theta_2,s_1)\dot{\theta}_1\dot{\theta}_2-\frac{1}{2}ks_1^2 \quad (7)$$

The components of the Lagrange function are;

$$m_{s_1}=\rho_1\int_0^{l_1}\phi_1^2dx_1+(m_{H_2}+m_2)a_h{}^2\gamma^2 \quad (8)$$

$$I_{t_1}=\rho_1\int_0^{l_1}(x_1+l_0)^2dx_1+I_{z_1}+(m_{H_2}+m_2)(2l_0+l_1) \quad (9)$$

$$I_{t_2}=m_2x^2{}_{CG_2}+I_{z_2} \quad (10)$$

$$m_{\dot{s}_1\dot{\theta}_1}=\rho_1\int_0^{l_1}\phi_1(x_1+l_0)dx_1(m_{H_2}+m_2)a_h\gamma(2l_0+l_1) \quad (11)$$

$$m_{\dot{s}_1\dot{\theta}_2}=c(\theta_2-\theta_1)m_2x_{CG_2}a_h\gamma \quad (12)$$

$$m_{\dot{\theta}_1\dot{\theta}_2}=s(\theta_2-\theta_1)x_{CG_2}a_h\gamma s_1+c(\theta_2-\theta_1)x_{CG_2}(2l_0+l_1) \quad (13)$$

$$k=EI_1\int_0^{l_1}\phi_1''^2dx_1 \quad (14)$$

The hybrid model cannot be expressed based solely on the angles of the links. In order to express flexibility, the generalized coordinate corresponding to the s1 vibration mode must also be taken into account. Thus, our model is expressed as three degrees of freedom.

$$q=\begin{bmatrix}\theta_1\\ \theta_2\\ s_1\end{bmatrix} \quad (15)$$

$$Q=\begin{bmatrix}\tau_1-\tau_2\\ \tau_2\\ -\tau_2a_h'\end{bmatrix} \quad (16)$$

The general form of the Lagrange equation is expressed as in Equation 17, $a_h=2+\frac{\pi^2}{2}$ $a_h'=\frac{\pi^2}{l_1}$

$$\frac{d}{dt}\left(\frac{\partial L}{\partial\dot{q}}\right)-\left(\frac{\partial L}{\partial q}\right)+\frac{\partial R}{\partial\dot{q}}=Q^T \quad (17)$$

The component denoted by R is the Rayleigh function that includes structural damping.

$$R=\frac{1}{2}c\dot{s}_1^2 \quad (18)$$

$$\ddot{\theta}_1=\frac{1}{\left(I_{t_1}+m_{s_1}s_1^2\right)}\begin{pmatrix}-m_{s_1}\dot{s}_1^2\dot{\theta}_1-m_{\dot{s}_1\dot{\theta}_1}\ddot{s}_1-\dot{m}_{\dot{\theta}_1\dot{\theta}_2}\dot{\theta}_2-m_{\dot{\theta}_1\dot{\theta}_2}\ddot{\theta}_2\\ +\frac{\partial m_{\dot{s}_1\dot{\theta}_2}}{\partial\theta_1}\dot{s}_1\dot{\theta}_2+\frac{\partial m_{\dot{\theta}_1\dot{\theta}_2}}{\partial\theta_1}\dot{\theta}_1\dot{\theta}_2+\tau_1-\tau_2\end{pmatrix} \quad (19)$$

$$\ddot{\theta}_2=\frac{1}{I_{t_2}}\begin{pmatrix}-\dot{m}_{\dot{s}_1\dot{\theta}_2}\dot{s}_1-m_{\dot{s}_1\dot{\theta}_2}\ddot{s}_1-\dot{m}_{\dot{\theta}_1\dot{\theta}_2}\dot{\theta}_1-m_{\dot{\theta}_1\dot{\theta}_2}\ddot{\theta}_1\\ +\frac{\partial m_{\dot{s}_1\dot{\theta}_2}}{\partial\theta_2}\dot{s}_1\dot{\theta}_2+\frac{\partial m_{\dot{\theta}_1\dot{\theta}_2}}{\partial\theta_2}\dot{\theta}_1\dot{\theta}_2+\tau_2\end{pmatrix} \quad (20)$$

$$\ddot{s}_1=\frac{1}{m_{s_1}}\begin{pmatrix}-m_{\dot{s}_1\dot{\theta}_1}\ddot{\theta}_1-\dot{m}_{\dot{s}_1\dot{\theta}_2}\dot{\theta}_2-m_{\dot{s}_1\dot{\theta}_2}\ddot{\theta}_2-m_{s_1}s_1\dot{\theta}_1^2\\ -ks_1-c\dot{s}_1+\frac{\partial m_{\dot{\theta}_1\dot{\theta}_2}}{\partial s_1}\dot{\theta}_1\dot{\theta}_2-a_h'\tau_2\end{pmatrix} \quad (21)$$

3. DYNAMICS

3.1 Dynamics Model of a Hybrid Manipulator

The dynamic model of an n-limb mechanical manipulator is defined by (Spong, 1993) as follows.

$$M(q)\ddot{q}+C(q,\dot{q})\dot{q}+G(q)=\tau \quad (22)$$

In the equation given in Equation (22), q is the generalized coordinate, τ is the applied torque, M(q) is the positive definite mass matrix, C(q) is the Coriolis expression and G(q) is the gravitational force vectors. Equation (22) is also expressed as follows;

$$Y(q,\dot{q},\ddot{q})\pi=\tau \quad (23)$$

π refers to inertia parameters, and Y refers to known functions of position, velocity and acceleration. Position and velocity errors are shown in Equation (24).

$$\tilde{q}=q-q_d \quad \text{and} \quad \dot{\tilde{q}}=\dot{q}-\dot{q}d \quad (24)$$

Using Equation (24), Equation (25) is obtained.

$$\dot{q}_r=\dot{q}_d-\Lambda\tilde{q} \quad \text{and} \quad \ddot{q}_r=\ddot{q}_d-\Lambda\dot{\tilde{q}} \quad (25)$$

Λ is a positive definite matrix. Control rule:

$$\tau_0=M_0(q)\ddot{q}_r+C_0(q,\dot{q})\dot{q}_r+G_0(q)-K\sigma$$
$$=Y(q,\dot{q},\dot{q}_r,\ddot{q}_r)\pi_0-K\sigma$$
(26)

$\pi0$ is the representation of nominal parameters. $K\sigma$ is the vector of the proportional-derivative (PD) controller.

$$\sigma=\dot{q}-\dot{q}_r=\dot{\tilde{q}}+\Lambda\tilde{q} \quad (27)$$

$$\tilde{\pi}=(\pi_0-\pi)\leq\rho \quad (28)$$

and

$$\|\tilde{\pi}\|=\|\pi_0-\pi\|\leq\delta \quad (29)$$

Additional control inputs u_1, u_2 and u_3 are defined in Equation (30). (Ozguney, 2017)

$$\tau=\tau_0+Y(q,\dot{q},\dot{q}_r,\ddot{q}_r)(u_1+u_2+u_3)=$$
$$Y(q,\dot{q},\dot{q}_r,\ddot{q}_r)(\pi_0+u_1+u_2+u_3)\text{-}K\sigma \quad (30)$$

If we write Equation (30) in Equation (29);

$$M(q)\dot{\sigma}+C(q,\dot{q})\sigma+K\sigma=Y(q,\dot{q},\dot{q}_r,\ddot{q}_r)(\pi_0-\pi)+u_1+u_2+u_3)$$
$$=Y(q,\dot{q},\dot{q}_r,\ddot{q}_r)(\tilde{\pi}+u_1+u_2+u_3)$$
(31)

Theorem 1:

$\alpha_1,\alpha_2,\ldots\alpha p$, $\beta_1,\beta_2,\ldots\beta p$ and $\lambda_1,\lambda_2\ldots,\lambda p\in R$, $\hat{\pi}_1$, $\dot{\hat{\rho}}_1$ and $\hat{\pi}_2$ terms define as follows; (Ozguney, 2017)

$$\hat{\pi}_1 = \begin{bmatrix} (\beta_1^2/\alpha_1)\dfrac{(1/\sqrt{2})\arctan(\tan(\alpha_1\int Y^T\sigma dt)_1/\sqrt{2})}{1+\cos^2(\alpha_1\int Y^T\sigma dt)_1} \\ (\beta_2^2/\alpha_2)\dfrac{(1/\sqrt{2})\arctan(\tan(\alpha_2\int Y^T\sigma dt)_2/\sqrt{2})}{1+\cos^2(\alpha_2\int Y^T dt)_2} \\ \cdots\cdots \\ (\beta_p^2/\alpha_p)\dfrac{(1/\sqrt{2})\arctan(\tan(\alpha_p\int Y^T\sigma dt)_p/\sqrt{2})}{1+\cos^2(\alpha_p\int Y^T\sigma dt)_p} \end{bmatrix} \tag{32}$$

$$\dot{\hat{\rho}}_1 = \Omega\left\|Y^T\sigma\right\| \tag{33}$$

$$\hat{\pi}_2 = \begin{bmatrix} \dfrac{\lambda_1}{1+\cos^2(\alpha_1\int Y^T\sigma dt)_1} \\ \dfrac{\lambda_2}{1+\cos^2(\int\alpha_2 Y^T\sigma dt)_2} \\ \cdots\cdot \\ \dfrac{\lambda_p}{1+\cos^2(\int\alpha_p Y^T\sigma dt)_p} \end{bmatrix} \tag{34}$$

u_1, u_2 and u_3 additional control inputs define as follows.

$$u_1 = \begin{cases} -\hat{\rho}_1\dfrac{Y^T\sigma}{\left\|Y^T\sigma\right\|} & \text{and} \quad \left\|Y^T\sigma\right\| > \varepsilon \\ -\hat{\rho}_1^2\dfrac{Y^T\sigma}{\varepsilon} & \text{and} \quad \left\|Y^T\sigma\right\| \le \varepsilon \end{cases}$$

$$u_2 = -\hat{\pi}_1$$

$$u_3 = \hat{\pi}_2 \tag{35}$$

Proof:

To ensure asymptotic tracking and robustness to uncertainties, a Lyapunov-based adaptive-robust controller is designed. The Lyapunov candidate is selected as follows.

Before defining the Lyapunov function, we need to define an error vector;

$$\tilde{\theta} = \hat{\pi}_1 - \hat{\pi}_2 \tag{36}$$

A positive definite Lyapunov function is defined: (Ozguney, 2017)

$$V(\sigma,\tilde{q},\tilde{\theta},(\hat{\rho}_1\text{-}\delta)) = \frac{1}{2}\sigma^T M(q)\sigma + \frac{1}{2}\tilde{q}^T B\tilde{q} + \frac{1}{2}\tilde{\theta}^T(\Psi+\Gamma^2)^2\tilde{\theta}$$
$$+\frac{1}{2}(\hat{\rho}_1-\delta)\Omega^{-1}(\hat{\rho}_1-\delta) + \frac{\varepsilon}{1} \ ;$$
$$V(\sigma,\tilde{q},\tilde{\theta}) \ge 0 \tag{37}$$

Ψ and Γ are measurable diagonal matrices. Ψ, takes constant values, Γ, can take changing values over time. Derivative of Lyapunov functions with respect to time is.

$$\dot{V} = \sigma^T M(q)\dot{\sigma} + \sigma^T\frac{1}{2}\dot{M}(q)\sigma + \tilde{q}^T B\dot{\tilde{q}}$$
$$+2\tilde{\theta}^T(\Psi+\Gamma^2)\Gamma\dot{\Gamma}\tilde{\theta} + \tilde{\theta}^T(\Psi+\Gamma^2)^2\dot{\tilde{\theta}} + (\hat{\rho}_1-\delta)\Omega^{-1}\dot{\hat{\rho}}_1 - \varepsilon \tag{38}$$

$B = 2\Lambda K$ and $\sigma^T[\dot{M}(q)\text{-}2C(q,\dot{q})]\sigma = 0 \ \ \forall\sigma\in R^n$, (Maouche and Atarri, 2009) and the time derivative of the Lyapunov function is;

$$\dot{V} = \text{-}\dot{\tilde{q}}^T K\dot{\tilde{q}}\text{-}\tilde{q}^T\Lambda K\Lambda\tilde{q} + \sigma^T Y(\tilde{\pi}+u_1) + (\hat{\rho}_1-\delta)\left\|Y^T\sigma\right\|$$
$$+\sigma^T Yu_2 + \sigma^T Yu_3 - \varepsilon + 2\tilde{\theta}^T(\Psi+\Gamma^2)\Gamma\dot{\Gamma}\tilde{\theta} + \tilde{\theta}^T(\Psi+\Gamma^2)^2\dot{\tilde{\theta}} \tag{39}$$

$$\dot{\hat{\rho}}_1 = \Omega\left\|Y^T\sigma\right\| \tag{40}$$

It is understood that there is a relation between, Ψ, Γ, u_2, u_3 and $\tilde{\theta}$. Ψ and Γ , p measurable diagonal matrix is defined as follows.

$$\Psi = \text{diag}(\frac{1}{\beta_i})$$

$$\Gamma = \text{diag}(\frac{\cos(\alpha_i\int Y^T\sigma dt)_i}{\sqrt{\beta_i}}) \tag{41}$$

$\tilde{\theta}$ defined as follows.

$$\tilde{\theta} = \hat{\pi}_1 - \hat{\pi}_2 = \begin{bmatrix} (\beta_1^2/\alpha_1)\dfrac{(1/\sqrt{2})\arctan(\tan(\alpha_1\int Y^T\sigma dt)_1/\sqrt{2}) - \lambda_1}{1+\cos^2(\alpha_1\int Y^T\sigma dt)_1} \\ (\beta_2^2/\alpha_2)\dfrac{(1/\sqrt{2})\arctan(\tan(\alpha_2\int Y^T\sigma dt)_2/\sqrt{2}) - \lambda_2}{1+\cos^2(\alpha_2\int Y^T dt)_2} \\ \cdots\cdots \\ (\beta_p^2/\alpha_p)\dfrac{(1/\sqrt{2})\arctan(\tan(\alpha_p\int Y^T\sigma dt)_p/\sqrt{2}) - \lambda_p}{1+\cos^2(\alpha_p\int Y^T\sigma dt)_p} \end{bmatrix}$$

$$\Psi + \Gamma^2, \tag{42}$$

$$\Psi + \Gamma^2 = \text{diag}(\frac{(1+\cos^2(\alpha_i\int Y^T\sigma dt)_i}{\beta_i}) \tag{43}$$

$\dot{\Gamma}$,

$$\dot{\Gamma} = \text{diag}(\frac{\text{-}\sin(\alpha_i\int Y^T\sigma dt)(\alpha_i Y^T\sigma)_i}{\sqrt{\beta_i}}) \tag{44}$$

and

$$\dot{\tilde{\theta}}_i = \frac{(\beta_i^2/\alpha_i)\dfrac{1+\tan^2(\alpha_i\int Y^T\sigma dt)_i}{2+\tan^2(\alpha_i\int Y^T\sigma dt)_i}}{1+\cos^2(\alpha_i\int Y^T\sigma dt)_1}(\alpha_i Y^T\sigma)_i$$
$$+\frac{2\cos(\alpha_i\int Y^T\sigma dt)_i\sin(\alpha_i\int Y^T\sigma dt)_i}{1+\cos^2(\alpha_i\int Y^T\sigma dt)_i}(Y^T\sigma)_i\tilde{\theta}_i \tag{45}$$

And the time derivative of the Lyapunov function is;

$$\dot{V} = -\dot{\tilde{q}}^T K \dot{\tilde{q}} - \tilde{q}^T \Lambda K \Lambda \tilde{q} + \sigma^T Y(\tilde{\pi} + u_1) + (\hat{\rho}_1 - \delta)\left\|Y^T\sigma\right\| + \sigma^T Y(u_2 + u_3) - \varepsilon + \tilde{\theta}^T \begin{bmatrix} \dfrac{\dfrac{1}{\cos^2(\alpha_1\int Y^T\sigma dt)_1}(1+\cos^2(\alpha_1\int Y^T\sigma dt)_1)}{1+\dfrac{1}{\cos^2(\alpha_1\int Y^T\sigma dt)_1}}(Y^T\sigma)_1 \\ \dfrac{\dfrac{1}{\cos^2(\alpha_2\int Y^T\sigma dt)_2}(1+\cos^2(\alpha_2\int Y^T\sigma dt)_2)}{1+\dfrac{1}{\cos^2(\alpha_2\int Y^T\sigma dt)_2}}(Y^T\sigma)_2 \\ \cdots\cdots \\ \dfrac{\dfrac{1}{\cos^2(\alpha_p\int Y^T\sigma dt)_p}(1+\cos^2(\alpha_p\int Y^T\sigma dt)_p)}{1+\dfrac{1}{\cos^2(\alpha_p\int Y^T\sigma dt)_p}}(Y^T\sigma)_p \end{bmatrix} \quad (46)$$

$\dfrac{1}{\cos^2(\int Y^T\sigma dt)} = 1 + \tan^2(\int Y^T\sigma dt)$ using this equation, $\dot{V}$ can be expressed as follows;

$$\begin{aligned} \dot{V} &= -\dot{\tilde{q}}^T K \dot{\tilde{q}} - \tilde{q}^T \Lambda K \Lambda \tilde{q} + \sigma^T Y(\tilde{\pi} + u_1) + (\hat{\rho}_1 - \delta)\left\|Y^T\sigma\right\| \\ &+ \sigma^T Y(u_2 + u_3) + \tilde{\theta} Y^T \sigma - \varepsilon \\ &= -\dot{\tilde{q}}^T K \dot{\tilde{q}} - \tilde{q}^T \Lambda K \Lambda \tilde{q} + \sigma^T Y(\tilde{\pi} + u_1) + (\hat{\rho}_1 - \delta)\left\|Y^T\sigma\right\| \\ &+ \sigma^T Y(u_2 + u_3) + \sigma^T Y(\hat{\pi} - \hat{\rho}_2) - \varepsilon \end{aligned} \quad (47)$$

$u_2 = -\hat{\pi}_1$ and $u_3 = -\hat{\pi}_2$, time derivative of the Lyapunov function is;

$$\dot{V} = -x^T Q x + (\sigma^T Y)^T(\tilde{\pi} + u_1) + (\hat{\rho}_1 - \delta)\left\|Y^T\sigma\right\| - \varepsilon \quad (48)$$

Assuming that, $x^T = [\tilde{q}^T, \dot{\tilde{q}}^T]$, $Q = \mathrm{diag}(\Lambda K \Lambda, K)$, it can be said that the first term of equation (48) is negative definite. Equation (48) is similar to the controller in (Spong, 1993) 's study. Therefore, the rest of the study will be similar to the study by (Spong, 1993)

Case 1:

If $\|Y^T\sigma\| > \varepsilon/p$ $\quad u_1 = -\hat{\rho}_1 \dfrac{Y^T\sigma}{\left\|Y^T\sigma\right\|}$ Equation (48) turns into Equation (49);

$$\begin{aligned} (Y^T\sigma)^T(\tilde{\pi} + u_1) + (\hat{\rho}_1 - \delta)\left\|Y^T\sigma\right\| - \varepsilon &= (Y^T\sigma)^T\tilde{\pi} - \delta\left\|Y^T\sigma\right\| - \varepsilon \\ &\le \left\|Y^T\sigma\right\|\{\|\tilde{\pi}\| - \delta\} - \varepsilon \\ &\le 0 \end{aligned} \quad (49)$$

Case 2:

If $\|Y^T\sigma\| \le \varepsilon/p$, $\quad u_1 = -\dfrac{\hat{\rho}_1^2}{\varepsilon} Y^T\sigma$ Equation (48) turns into Equation (50);

$$\begin{aligned} &(Y^T\sigma)^T(\tilde{\pi} + u_1) + (\hat{\rho}_1 - \delta)\left\|Y^T\sigma\right\| - \varepsilon \\ &= (Y^T\sigma)^T\tilde{\pi} - \frac{\hat{\rho}_1^2}{\varepsilon}\left\|Y^T\sigma\right\|^2 + \hat{\rho}_1\left\|Y^T\sigma\right\| - \delta\left\|Y^T\sigma\right\| - \varepsilon \\ &\le \left\|Y^T\sigma\right\|\{\|\tilde{\pi}\| - \delta\} - \frac{\hat{\rho}_1^2}{\varepsilon}\left\|Y^T\sigma\right\|^2 + \{\hat{\rho}_1\left\|Y^T\sigma\right\| - \varepsilon\} \\ &\le 0 \end{aligned} \quad (50)$$

$\|\tilde{\pi}\| \le 0$ and $\left\|Y^T\sigma\right\| \le \varepsilon / \hat{\rho}_1$

$$\dot{V} \le -xQx \quad (51)$$

4. CONTROLLER

4.1 Application the adaptive-robust controller to hybrid robot manipulator

If the torque equations obtained using Equation (19), Equation (20), and Equation (21) are arranged in matrix format;

$$\begin{bmatrix} M_{11} & M_{12} & M_{13} \\ M_{21} & M_{22} & M_{23} \\ M_{31} & M_{32} & M_{33} \end{bmatrix}\begin{bmatrix} \ddot{\theta}_1 \\ \ddot{\theta}_2 \\ \ddot{s}_1 \end{bmatrix} + \begin{bmatrix} C_{11} & C_{12} & C_{13} \\ C_{21} & C_{22} & C_{23} \\ C_{31} & C_{32} & C_{33} \end{bmatrix}\begin{bmatrix} \dot{\theta}_1 \\ \dot{\theta}_2 \\ \dot{s}_1 \end{bmatrix}\begin{bmatrix} G_{11} & G_{12} & G_{13} \\ G_{21} & G_{22} & G_{23} \\ G_{31} & G_{32} & G_{33} \end{bmatrix}\begin{bmatrix} \theta_1 \\ \theta_2 \\ s_1 \end{bmatrix} = \begin{bmatrix} \tau_1 - \tau_2 \\ \tau_2 \\ -\tau_2 a_h' \end{bmatrix} \quad (52)$$

$$\begin{bmatrix} -\left(I_{t_1} + m_{s_1}s_1^2\right) & m_{\dot{\theta}_1\dot{\theta}_2} & -m_{\dot{s}_1\dot{\theta}_1} \\ -m_{\dot{\theta}_1\dot{\theta}_2} & -I_{t_2} & -m_{\dot{s}_1\dot{\theta}_2} \\ -m_{\dot{s}_1\dot{\theta}_1} & m_{\dot{s}_1\dot{\theta}_2} & -m_{s_1} \end{bmatrix}\begin{bmatrix} \ddot{\theta}_1 \\ \ddot{\theta}_2 \\ \ddot{s}_1 \end{bmatrix}$$

$$\begin{bmatrix} -\left(m_{s_1}\dot{s}_1^2\right) + \dfrac{\partial m_{\dot{\theta}_1\dot{\theta}_2}}{\partial\theta_1}\dot{\theta}_2 & -m_{\dot{\theta}_1\dot{\theta}_2} + \dfrac{\partial m_{\dot{s}_1\dot{\theta}_2}}{\partial\theta_1}\dot{s}_1^2 & 0 \\ -\dot{m}_{\dot{\theta}_1\dot{\theta}_2} + \dfrac{\partial m_{\dot{\theta}_1\dot{\theta}_2}}{\partial\theta_2}\dot{\theta}_2 & \dfrac{\partial m_{\dot{s}_1\dot{\theta}_2}}{\partial\theta_2}\dot{s}_1 & -\dot{m}_{\dot{s}_1\dot{\theta}_2} \\ -m_{s_1}s_1\theta_1 + \dfrac{\partial m_{\dot{\theta}_1\dot{\theta}_2}}{\partial s_1}\dot{\theta}_2 & -\dot{m}_{\dot{s}_1\dot{\theta}_2} & -c \end{bmatrix}\begin{bmatrix} \dot{\theta}_1 \\ \dot{\theta}_2 \\ \dot{s}_1 \end{bmatrix}$$

$$\begin{bmatrix} 0 & 0 & 0 \\ 0 & 0 & 0 \\ 0 & 0 & -k \end{bmatrix}\begin{bmatrix} \theta_1 \\ \theta_2 \\ s_1 \end{bmatrix} \quad (53)$$

π values are defined in Equation (54).

$$\begin{aligned} \pi_1 &= \rho_1\int_0^{l_1}(x_1 + l_0)^2 dx_1 + I_{z_1} + (m_{H_2} + m_2)(2l_0 + l_1) \\ \pi_2 &= \rho_1\int_0^{l_1}\phi_1^2 dx_1 + (m_{H_2} + m_2)a_h{}^2\gamma^2 \\ \pi_3 &= \rho_1\int_0^{l_1}\phi_1(x_1 + l_0)dx_1(m_{H_2} + m_2)a_h\gamma(2l_0 + l_1) \\ \pi_4 &= x_{CG_2}a_h\gamma \\ \pi_5 &= x_{CG_2}(2l_0 + l_1) \\ \pi_6 &= m_2 x_{CG_2}a_h\gamma \\ \pi_7 &= m_2 x^2{}_{CG_2} + I_{z_2} \\ \pi_8 &= EI_1\int_0^{l_1}\phi_1''^2 dx_1 \\ \pi_9 &= 2\delta w_n m_{s_1} \end{aligned} \quad (54)$$

The parameters of the flexible link robot are given in Appendix A.

To apply the proposed control law, the parameter uncertainties must first be defined. Two different approaches were considered for this purpose. The mass of the second link (m_{l2}) is given as 0.0586 kg. In the first approach, this mass was doubled, and the lengths of both the first and second links were increased by 50%. The corresponding parameter values for this case are provided in Appendix B.

Figure 2 shows the trajectory applied to the system. A step trajectory with an amplitude of 0.01 was applied to the system.

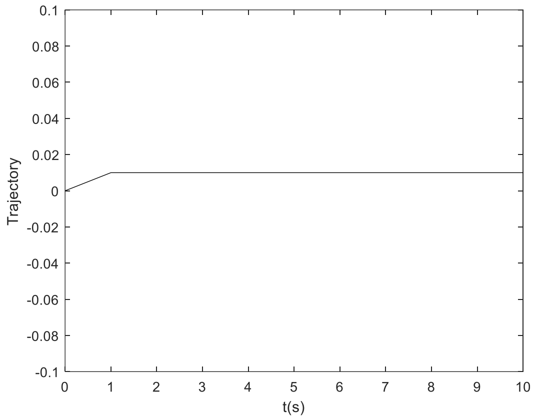

Fig. 2. Trajectory.

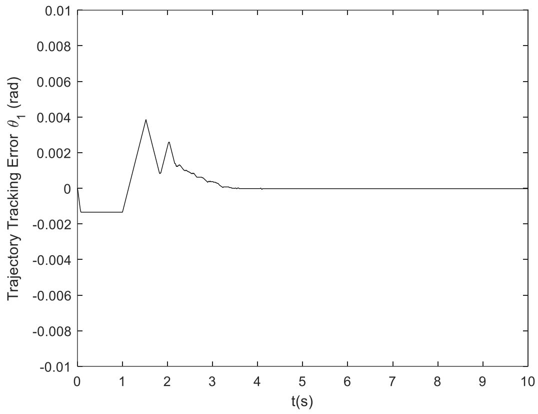

(a)

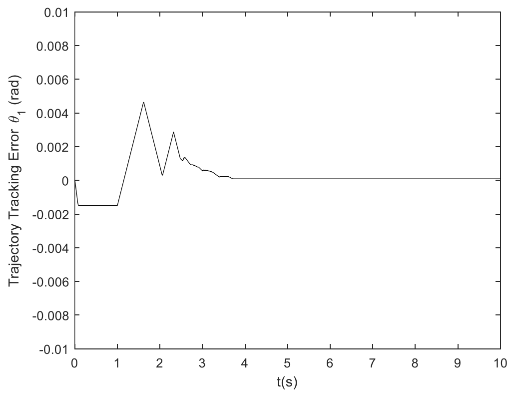

(b)

Fig. 3. Trajectory tracking error of angle in step orbit with amplitude of 0.01. (Λ=diag(100 100 100), K= diag(100 100 100), α=10, β=0.01, λ=0.1, ε=1, Ω=0.001).

Figure 3 illustrates the variation of the joint angle over time. Two subfigures, (a) and (b), are presented. In subfigure (a), a trajectory with an amplitude of 0.01 was applied, whereas in subfigure (b), an external disturbance of the same amplitude was added to the applied trajectory. As observed in the figure, when no external disturbance is present, the maximum trajectory tracking error is approximately 0.004 radians. Under the influence of external disturbances, the system exhibits a slight delay in reaching this maximum error. In both cases, the trajectory tracking error rapidly converges to zero, demonstrating the robustness of the controller even in the presence of external disturbances.

Figure 4 illustrates the variation of the joint angle over time. Two subfigures, (a) and (b), are presented. In subfigure (a), a trajectory with an amplitude of 0.01 was applied, while in subfigure (b), an external disturbance of the same amplitude was added to the applied trajectory. As shown in the figure, when no external disturbance is present, the maximum trajectory tracking error is approximately 0.002 radians. Under the influence of external disturbances, the system exhibits a slight delay in reaching this maximum error. In both cases, the trajectory tracking error rapidly converges to zero, demonstrating the effectiveness of the control approach.

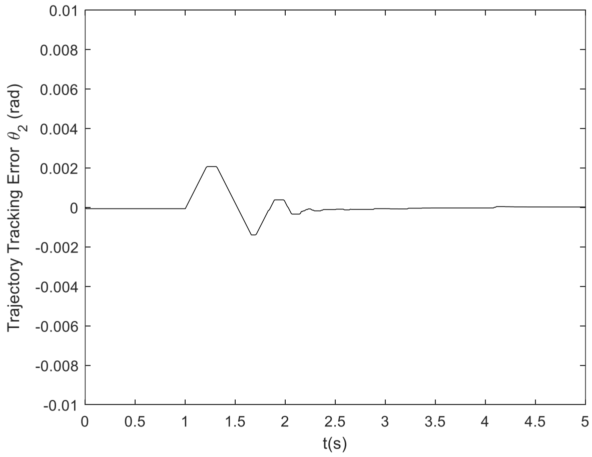

(a)

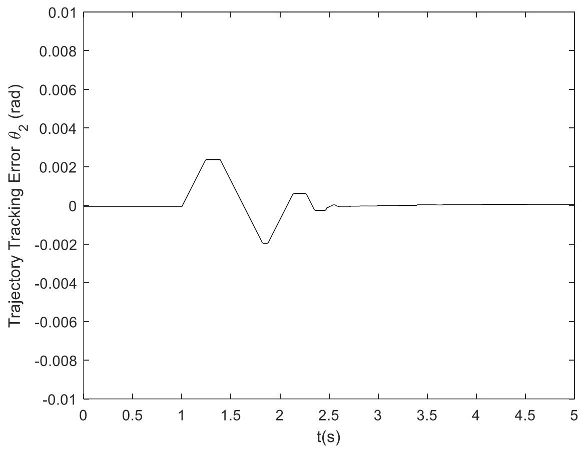

(b)

Fig. 4. Trajectory tracking error of angle in step orbit with amplitude of 0.01. (Λ=diag(100 100 100), K= diag(100 100 100), α=10, β=0.01, λ=0.1, ε=1, Ω=0.001).

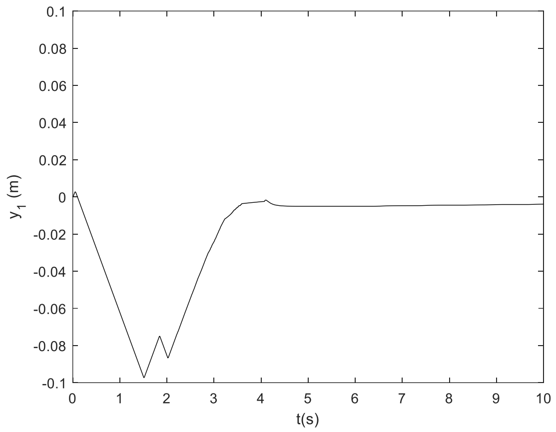

(a)

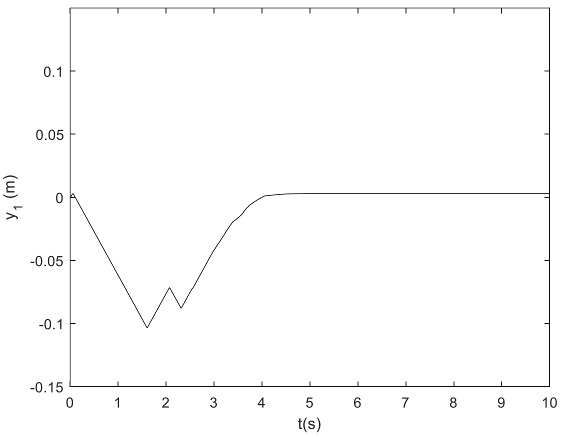

(b)

Fig. 5. Time-dependent variation of y1 deviation in step trajectory with amplitude of 0.01. (Λ=diag(100 100 100), K= diag(100 100 100), α=10, β=0.01, λ=0.1, ε=1, Ω=0.001).

Figure 5 shows the variation of elastic deflection over time. There are two shapes (a) and (b). In (a) a trajectory with only 0.01 amplitude was applied, in (b) an external factor of the same amplitude was applied in addition to the applied trajectory. With a maximum deviation of 0.1 meter, the link returns to its original position after 5 seconds. It can be said that the elastic deflection value is a very good result for flexible systems. When examined for both cases, it is observed that the amount of deviation is very close to each other and is minimized quickly.

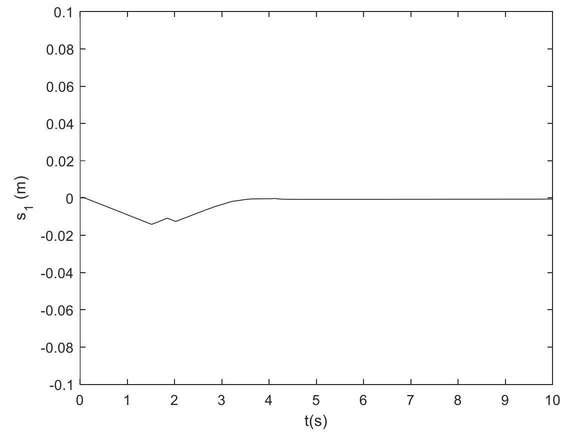

(a)

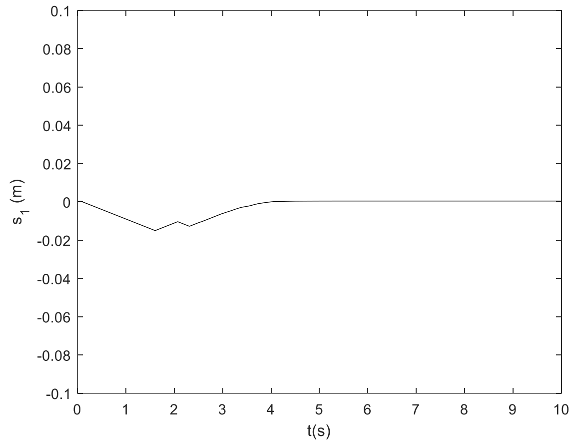

(b)

Fig. 6. Time-dependent variation of s1 mode in step trajectory with amplitude of 0.01. (Λ=diag(100 100 100), K= diag(100 100 100), α=10, β=0.01, λ=0.1, ε=1, Ω=0.001).

The mode represents the motion characteristics of the robot. To determine the deviation in a flexible-link robot, the eigenfunctions and mode shapes of the governing equation are required. Since it is generally difficult to obtain exact eigenfunctions, the accepted mode method was employed, where eigenfunctions of another function satisfying similar boundary conditions were used as approximations. To simplify the system, only the first mode was considered in the analysis. Figure 6 illustrates the time-dependent variation of the s_1 mode. Two subfigures, (a) and (b), are presented. In subfigure (a), a trajectory with an amplitude of 0.01 was applied, whereas in subfigure (b), an external disturbance of the same amplitude was applied in addition to the trajectory. It can be observed that similar results were obtained in both cases.

Figure 7 shows the control force applied to the first link. When both situations are examined, it is understood that the system can be controlled easily with small force. It seems that the system works properly by applying a little more force than normal to absorb external disturbances.

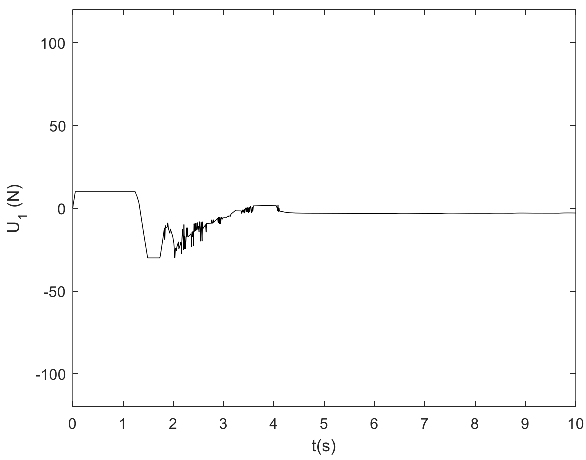

(a)

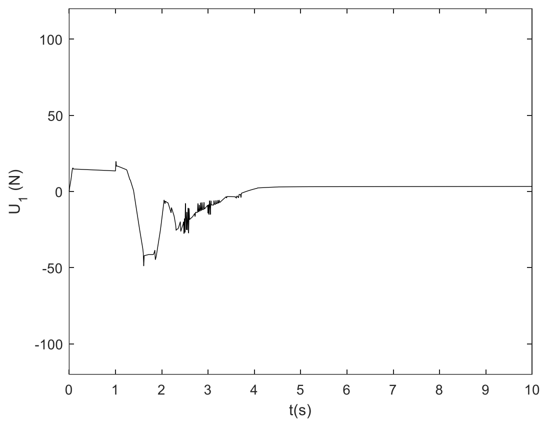

(b)

Fig. 7. Time-dependent variation of the u1 controller force in a step trajectory with an amplitude of 0.01. (Λ=diag(100 100 100), K= diag(100 100 100), α=10, β=0.01, λ=0.1, ε=1, Ω=0.001).

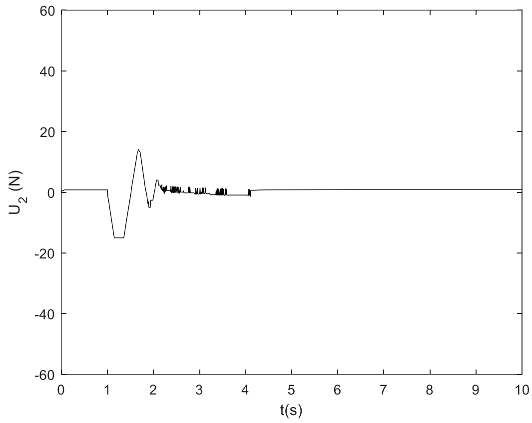

(a)

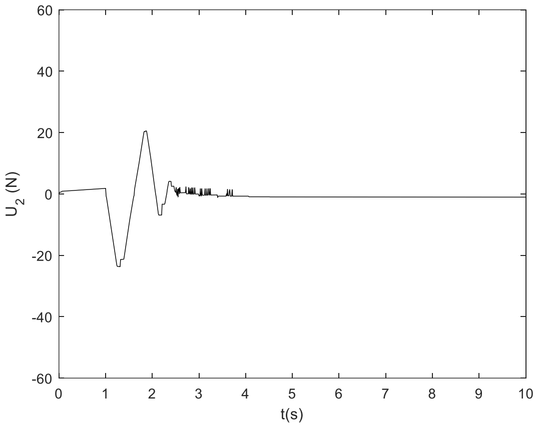

(b)

Fig. 8. Time-dependent variation of the u2 controller force in a step trajectory with an amplitude of 0.01. (Λ=diag(100 100 100), K= diag(100 100 100), α=10, β=0.01, λ=0.1, ε=1, Ω=0.001).

Figure 8 shows the time-dependent change of the control force applied to the rigid link. By applying less force than the elastic link, the system is ensured to work properly. A similar trend is observed in both cases.

5. CONCLUSIONS

This study presents a novel adaptive-robust control strategy specifically designed for hybrid manipulators consisting of both flexible and rigid links. Unlike traditional approaches that treat rigid and flexible systems separately, our method integrates the control of both link types within a unified framework. Robots with elastic links, which are widely used especially in the production sector, are modeled here as a hybrid system with a flexible first link and a rigid second link. The control law has been redesigned to address the unique dynamic challenges posed by this hybrid structure, aiming to minimize deviation in the elastic link and ensure that the trajectory tracking error approaches zero.

When the proposed controller is applied to the model, simulation results confirm its effectiveness and robustness against parameter uncertainties and external disturbances. Notably, the trajectory tracking error converges to zero even under additional disturbance inputs, demonstrating the success of the approach. For future studies, alternative control laws may be developed, or optimal performance could be achieved by selecting suitable controller parameters tailored to specific applications.

ACKNOWLEDGEMENTS

This research did not receive any specific grant from funding agencies in the public, commercial, or not-for-profit sectors.

REFERENCES

Akyuz, I.H, Kizir, S., Bingul, Z. (2010) Tek eklemli esnek bağlı robot kolunun modellenmesi, tasarımı ve bulanık mantık ile kontrolü, 558–564. *Otomatik Kontrol Ulusal Toplantısı*, Gebze Kocaeli,

Book, W.J. (1990). Modeling design and control of flexible manipulator arms: A tutorial review. 500-506. *29-th IEEE Conference on Decision and Control*. 5-7 Dec. Honolulu USA.

Chen, W. (2001). Dynamic modeling of multi-link flexible robotic manipulators. *Computers and Structures*. 79,183-195.

Chen, S., He, W., Zhao, Z., Feng, Y., Liu, Z., Hong, K.-S. (2025). Adaptive control of a flexible manipulator with unknown hysteresis and intermittent actuator faults. *IEEE/CAA Journal of Automatica Sinica*, 12(1), 145–158.

Choi, S.B., Cheong, C.C., Shin, H.C. (1995). Sliding mode control of vibration in a single-link flexible arm with parameter variations. *Journal of Sound and Vibration*. 179(5), 737-748.

Dwivedy, S.K., Eberhard, B., (2006). Dynamic analysis of flexible manipulators, a literature review. *Mechanism and Machine Theory*.;41(2006), 749–777.

Gee, S.S., Lee, T.H., Zhug, G.A., (1997) Nonlineer feedback controller for a single link flexible manipulator based on a finite element method. *Journal of Robotic Systems*. 14(3), 165-178.

Hayta, U., Kapucu, S., Yesil, E. (2013). PI type fuzzy controller for position control of flexible manipulators. *16. National Machine Theory Symposium*. 564-569, 12-13 Sept. 2013, Erzurum Turkey.

Khairudin, M., Mohamed, Z., Husain, A.R., Ahmad, M.A., Dynamic modelling and characterization of a two-link flexible robot manipulator. (2010). *Journal of Low Frequency Noise, Vibration and Active Control*. 29(3),207-209.

Li, L., Liu, J. (2023). Nussbaum function-based adaptive boundary control for flexible manipulator with unknown control directions and nonlinear time-varying actuator faults. *International Journal of Robust and Nonlinear Control*, 33(15), 7753–7770.

Mallikarjunaıah, S., Reddys, S.N., (2013). Design of PID controller for flexible link manipulator. International *Journal of Engineering Research and Applications*. 3(1),1207-1212.

Maouche AR, Attari M. CMAC based adaptive control of a flexible link manipulator. *35th Annual Conference of IEEE Industrial Electronics*. 3-5 Nov. 2009, Porto, Portugal, 1480-1485.

Ma, X., Liu, J. (2024). Adaptive contact-force control and vibration suppression for constrained flexible manipulator with unknown control direction and time-varying actuator fault. *Journal of Vibration and Control*, 30(2), 342–357.

Ozguney, O.C. Hybrid Control of Mechanical Systems. (*PhD thesis*, 2017). Istanbul University, Istanbul.

Spong, M.W., (1993) Adaptive control of robot manipulators: design and robustness. 2826-2830. In 1993 *AmericanControl Conference*. 4 June 1993, San Francisco, CA, United States.

Wit, J.D., (2014). Modelling and control of a two-link flexible manipulator. *Master Thesis*, 2014, Eindhoven University of Technology.

Yağız, N., Yüksek, İ., Kepçeler, B., (2001). Sliding mode control of a planar flexible single-arm robot. *Journal of Polytechnic*. 4(2),15-19.

Appendix A. FIRST APPENDIX

Table 1. Parameters of flexible link robot (Wit, 2014).

ρ_1	Density of first link	0.7597	kgm^{-1}
ρ_2	Density of second link	0.2662	kgm^{-1}
l_0	Length of the motor	0.06465	M
l_1	Length of the first link	0.22	M
l_2	Length of the second link	0.22	M
m_{H2}	Mass of second hub	0.593	Kg
m_{mb2}	Mass of second mounting bracket	0.4036	Kg
m_{l2}	Length of the second link	0.0586	Kg
EI_1	Bending stiffness	2.69	Nm^2
I_{z1}	Moment of inertia	0.0007424	Kgm^2
I_{z2}	Moment of inertia	0.0004456	Kgm^2
ρ_1	Density of first link	0.7597	kgm^{-1}
ρ_2	Density of second link	0.2662	kgm^{-1}
l_0	Length of the motor	0.06465	M
l_1	Length of the first link	0.22	M
l_2	Length of the second link	0.22	M
m_{H2}	Mass of second hub	0.593	Kg
m_{mb2}	Mass of second mounting bracket	0.4036	Kg
m_{l2}	Length of the second link	0.0586	Kg
EI_1	Bending stiffness	2.69	Nm^2
I_{z1}	Moment of inertia	0.0007424	Kgm^2
I_{z2}	Moment of inertia	0.0004456	Kgm^2

Appendix B. SECOND APPENDIX

Table 2. $\tilde{\pi}$ values.

$\tilde{\pi}_1$	$\tilde{\pi}_2$	$\tilde{\pi}_3$	$\tilde{\pi}_4$	$\tilde{\pi}_5$	$\tilde{\pi}_6$	$\tilde{\pi}_7$	$\tilde{\pi}_8$	$\tilde{\pi}_9$
0.3720	10.4	0.846	0.33	0.01	0.144	0.0011	20509	10.41